Interaction Dynamics of Elastic Waves with a Complex Nonlinear Scatterer through the Use of a Time Reversal Mirror

T. J. Ulrich,[1] Paul A. Johnson,[1] and Robert A. Guyer[2,1]

[1]*EES Division, Geophysics Group, Los Alamos National Laboratory, Los Alamos, New Mexico 87545, USA*

[2]*Department of Physics, University of Massachusetts, Amherst, Massachusetts 07030, USA*

(Received 14 July 2006; published 7 March 2007)

This Letter reports on work performed to locate and interrogate a nonlinear scatterer in a linearly elastic medium through the use of a time reversal mirror in combination with nonlinear dynamics. Time reversal provides the means to spatially and temporally localize elastic energy on a scattering feature while the nonlinear dynamics spectrum allows one to determine whether the scatterer is nonlinear (e.g., mechanical damage). Here elastic waves are measured in a solid and processed to extract the nonlinear elastic response. The processed elastic signals are then time reversed, rebroadcast, and found to focus on the nonlinear scatterer, thus defining a time-reversed nonlinear elastic wave spectroscopy process. Additionally, the focusing process illuminates the complexity of the nonlinear scatterer in both space and time, providing a means to image and investigate the origins and physical mechanisms of the nonlinear elastic response.

DOI: 10.1103/PhysRevLett.98.104301 PACS numbers: 43.25.+y, 62.30.+d

The interaction physics of an elastic wave with a nonlinear scatterer in a solid is a fascinating and extremely complex process. The scattering process induces localized wave distortion and simultaneous nonlinear wave mixing, producing wave harmonics and intermodulation (e.g., [1]). A nonlinear scatterer could be localized, e.g., a crack, a delamination, thermal damage in an otherwise elastically linear material. It could be present uniformly in a material having distributed nonlinear scatterers, such as in a rock sample, some ceramics, and some metals (e.g., [1,2]). The presence of nonlinear scattering is an extremely sensitive diagnostic for the presence of mechanical damage [2–4]. However, few measurements exist that directly image the nonlinear scatterer or see the dynamics of the scattering process. Such measurements are difficult to conduct. One of the few examples we are aware of is Kazakov *et al.* [5] (and in unpublished data) in which the geometry of the sample, a thin metal plate, allowed one to ''image'' a crack through a time windowing of a modulated signal. These authors found significant nonlinear scattering near the crack center and at the crack tips.

The interaction physics of a nonlinear scatterer and an elastic wave are interesting from another perspective. For example, we know that a crack is a nonlinear scatterer but we do not understand the physical nature of the nonlinear scattering process (e.g., [1,3,6]). Simple models treat a crack as a rectifier; i.e., a crack can transmit compression but not tension. Thus an elastic wave incident of the crack is rectified, generating elastic wave components at the harmonics at $2f, 3f, 4f \ldots nf$. This simple model for the nonlinear dynamics of a crack has had success in describing a certain class of nonlinear scattering such as delaminations in composite materials [7,8] but does not work universally for the general complexity of thermal damage, complex cracks, and other complex nonlinear scatterers. Unraveling a crack's behavior will require experimental probes that can directly and actively disturb it and watch its response. The experiment reported here, combining a time reversal mirror [9] and nonlinear scattering, a technique termed time-reversed nonlinear elastic wave spectroscopy (TR NEWS), is a first step in this direction.

The purpose of this Letter is to illustrate a method for locating and interrogating a nonlinear scatterer. This method employs a time reversal mirror to detect and rebroadcast signals that have their source at the nonlinear scatterer. The breakdown of time reversal in a nonlinear medium has been considered [10]; however, as the propagation medium remains linearly elastic (i.e., the nonlinear scattering is highly localized) there are no issues of breaking time reversal invariance. The essential elements of the principle behind the method are contained in a one-dimensional model. For a longitudinal plane wave, propagating in a bounded medium, $0 < x < L$, having no attenuation, the equation of motion is [11,12]

$$\frac{1}{c^2}\frac{\partial^2 u(x,t)}{\partial t^2} - \frac{\partial^2 u(x,t)}{\partial x^2} = \frac{\partial}{\partial x}\left(\beta(x)\left[\frac{\partial u(x,t)}{\partial x}\right]^2\right) + S_{\mathrm{lo}}(0,t) + S_{\mathrm{hi}}(L,t), \quad (1)$$

where $u(x,t)$ is the particle displacement, c is the wave speed, $\beta = \beta_0\delta(x-a)$ is a localized classical nonlinearity, and S_{lo} and S_{hi} are sources (placed at the medium surfaces) having frequencies f_{lo} and f_{hi}, respectively, and amplitudes A_{lo} and A_{hi}, respectively. When the sources are turned on momentarily near $t = 0$, two displacement fields are launched into the system, u_{lo} and u_{hi}, which on simultaneous arrival at $x = a$ mix and become the source of broadcast from a at frequencies $f_{\pm} = f_{\mathrm{hi}} \pm f_{\mathrm{lo}}$ with amplitude $S_a(t) \propto \beta_0 u_{\mathrm{lo}}(a,t)u_{\mathrm{hi}}(a,t) \propto \beta_0 A_{\mathrm{lo}}A_{\mathrm{hi}}$. The Green functions $G(x,t|a,t')$ carry $S_a(t')$ to a set of detectors at $x = b_i$, $i = 1 \cdots M$, where it is received as $r_i(t)$ and recorded. These recorded signals are filtered around fre-

quency $f_+(f_-)$, time reversed, and rebroadcast as $s_i(t)$ from b_i, $i = 1 \cdots M$ simultaneously. The Green functions $G(x, t|b_i, t')$ carry the $s_i(t')$ to $x = a$, the purported source of $f_+(f_-)$, where they reassemble. As a last step a test of this reassembly is conducted. Throughout, the nonlinearity works only at the moments of time when $u_{\mathrm{lo}}(a, t)u_{\mathrm{hi}}(a, t)$ is of sufficient amplitude to contribute to $S_a(t)$; i.e., $G(x, t|a, t')$ is elastically linear. This scenario differs from conventional use of time reversal mirrors in that the source, the nonlinear scatterer, with known amplitude structure, $S_a(t) \propto \beta_0 A_{\mathrm{lo}} A_{\mathrm{hi}}$, has unknown time structure. It should be noted that the method described herein utilizes only one type of nonlinear response; however, a similar technique can be used for any nonlinear signal originating from a localized nonlinear scatterer.

The above scenario is realized experimentally in the following manner: the sample, a steel automotive bearing cap (Fig. 1), is excited from $t = 0$ simultaneously with a broadband impulse (which excites its low frequency normal modes, e.g., $f_{\mathrm{lo}} = 4$ kHz) and a narrowband high frequency tone burst (200 cycles at $f_{\mathrm{hi}} = 204$ kHz). At the site of a nonlinear scatterer in the sample, the low frequency mode(s) and the high frequency tone burst are mixed and broadcast at frequencies $f_\pm$ and possibly others. The elastic response of the sample is recorded from $0 \leq t \leq t_1$ at 6 different locations on the sample surface using piezoelectric ceramic disks (PZT-5A, 1 cm diameter, 2 mm thick) bonded to the sample with epoxy (Devcon 2-ton). The signal recorded by each ceramic disk, a normal displacement at the surface, is Fourier analyzed to determine the spectral composition of the response (Fig. 2). Each of the 6 recorded signals is filtered about a frequency prominent in the response, i.e., $f_\pm$, time reversed, and rebroadcast at a moment of time denoted t_R. We expect these rebroadcast signals to focus on their source, the nonlinear scatterer.

We use a sample having a known nonlinear scatterer (a 1 cm long $\times$ 0.5 cm deep "hairline" crack) that intersects the sample surface in the arch. Following rebroadcast of the time reversed, filtered signals we detect the particle velocity on the surface of the sample, $U(x_{ij}, t)$ [$x_{i,j} = (x_0 + i\Delta X, y_0 + j\Delta Y)$, $i = 1 \cdots 25$, $j = 1 \cdots 25$, $\Delta X =$ 1.0 mm, and $\Delta Y = 0.8$ mm] with a scanning laser vibrometer system (Polytec 3001, 125 mm/s/V). Typically in time reversal experiments, the source of the signal to be time reversed is sharply defined in time (e.g., a delta function or single period sinusoid). Here the source is of unknown temporal structure; it is due to the mixing of the two primary sources as they visit (and revisit through scattering) the site of the nonlinear scatterer. Without knowledge of the form or timing of this source we can neither define an initial source time nor anticipate a time of focus. To obviate this difficulty we assume that the amount of energy delivered to a point x_{ij} on the surface, over a time interval Δt at t_k, will be proportional to the strength of the focused signal at (x_{ij}, t_k), where t_k is measured from the moment of rebroadcast, t_R. We calculate an energy from the displacement amplitudes $U(x_{ij}, t_k)$ using

$$E(x_{ij}, t_k) = \frac{1}{\Delta t} \int_{t_k}^{t_k + \Delta t} U^2(x_{ij}, t_k + \tau) d\tau. \qquad (2)$$

The primary data we report are $E(x_{ij}, t_k)$.

All experiments are performed on two nominally identical samples, same geometry, wave speed ($v_p = 3325$ m/s),

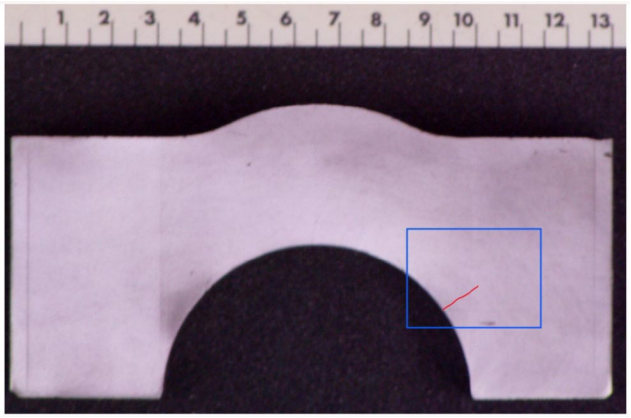

FIG. 1 (color online). Bearing cap sample photograph. Sample is composed of a low carbon steel, $c = 3325$ m/s, with dimensions $\sim$13.5 cm $\times$ 6.5 cm $\times$ 3.0 cm. The rectangle indicates the approximate scan area for which results are presented in Figs. 3 and 4 (identical area for both nonlinear and linear samples). The crack is artificially highlighted in red to enhance its visibility. PZT transducers were mounted to the opposing face and two ends (i.e., right and left perpendicular faces). The broadband impulse was initiated at the top center on the convex portion of the arch.

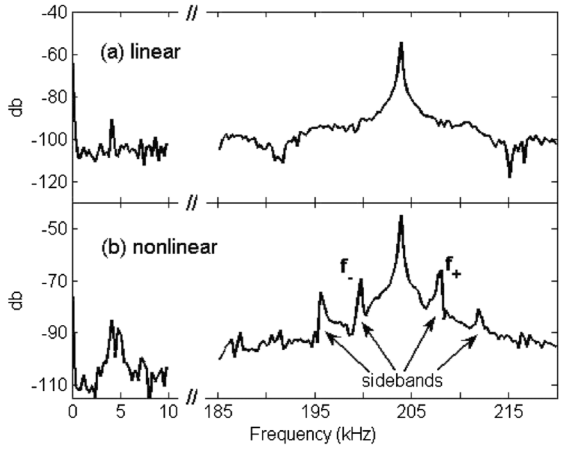

FIG. 2. (a) Power spectrum from an elastically linear (undamaged) sample indicating no wave mixing between the low and high frequency signals. (b) Power spectrum from an elastically nonlinear (mechanically damaged) sample showing the mixing of a high frequency puretone (204 kHz) with a low frequency (4 kHz) normal mode. The samples are identical (i.e., geometry, transducer locations, wave speed, etc.) with the exception of the presence of a $\sim$1 cm crack in the nonlinear sample (illustrated in Figs. 1, 3, and 4).

and employing identical transducers identically situated. The samples differed in that one had a surface intersecting crack that we explore. In Fig. 3 we show the rebroadcast signals detected by the laser vibrometer in the vicinity of the crack, integrated as in Eq. (2) over 3.277 ms following rebroadcast. In Figs. 3(a) and 3(b) are results for two different sideband frequencies, in Fig. 3(c) is the result for an arbitrary frequency unrelated to nonlinear mixing, and in Fig. 3(d) we show the result from the identical scan region of the linear elastic (undamaged) sample. For rebroadcast at $f_+ \approx 208$ kHz (a) and at $f_- \approx 200$ kHz (b) there is energy focusing near the crack (white line). This is in contrast to using a time-reversed signal filtered about an arbitrary frequency ($f_{\text{arb}} = 108$ kHz) (c) and the linear sample (d) each of which show no evidence of such focusing. Study of the amplitude dependence of the filtered received signals confirms the anticipated amplitude dependence, $r_i(t) \propto A_4 A_{204}$.

The difference in the details in the focusing in Figs. 3(a) and 3(b) indicates that different sideband frequencies may have different origins in space and time; i.e., the nonlinear scatterer is a complex elastic system. To look in some detail at the focusing process we define a narrow time window, $\Delta t = 0.062$ ms, which we set at 105 equally spaced, overlapping time points over a 3.277 ms time interval starting from t_R. We calculate the energy for each window as in Eq. (2) for the case shown in Fig. 3(b). Selected results of this moving window energy analysis are shown in Fig. 4 for 3 times, t_k, measured from t_R. Results for all 105 moments of time can be seen as a video, as well as similar videos for other frequencies in both the linear and nonlinear samples [13]. The focusing is spatially variable [Fig. 4(b) and 4(c)] being primarily at the two ends of the crack. Moreover, the focusing has periodicity of approximately 1 kHz with a phase difference between the behavior at the two crack ends. One interpretation of this phenomenon is that the nonlinear scatterer broadcasts at multiple times from the two distinct regions of the scatterer. Focusing events between the ends are at much smaller amplitudes and without apparent periodicity. The regions of apparent nonlinear scattering (i.e., the crack opening and crack tip) are not surprising as it is well known from fracture mechanics that stress concentrations are high at the tips of cracks, while the crack opening (i.e., the end of the crack at the arched free boundary) is logically the most mobile and thus easily excitable.

This work illustrates that a nonlinear scatterer can be isolated applying the TR NEWS method illustrated here, and that the spatial and temporal complexity may be imaged. Here we are able to explore the spatial-temporal nature of nonlinear scattering from a mechanical damage feature. This interrogation of the dynamical response of a nonlinear feature to an elastic wave may provide the details necessary to construct constitutive models of crack-wave

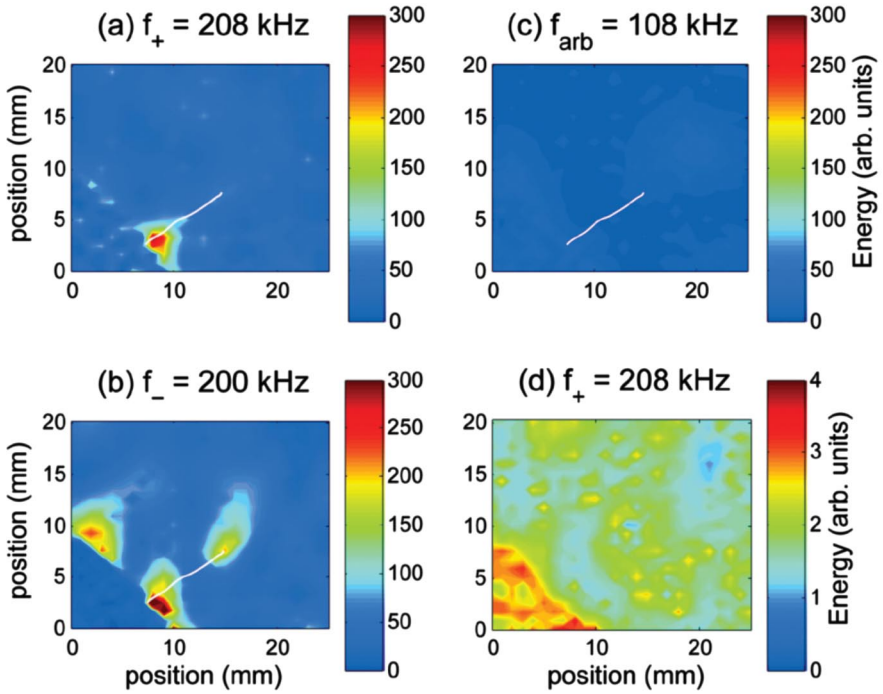

FIG. 3 (color). Elastic energy [as calculated from Eq. (2)] localization in the elastically nonlinear sample from rebroadcasting the time-reversed signal filtered about (a) $f_+ = 208$ kHz, (b) $f_- = 200$ kHz, and (c) $f_{\text{arb}} = 108$ kHz. The crack highlighted in white has been overlayed to show its location. Notice the difference in spatial focusing of the elastic energy depending on the sideband frequency used, as well as the lack of focusing of f_{arb}. (d) For comparison, the energy in a elastically linear sample is shown when filtering for $f_+ = 208$ kHz in the time-reversed signal. Note the lack of focusing of energy, emphasized by the smaller energy-scale interval in comparison to both (c) and (d). The curved feature in the lower left portion of (a)–(d) and Fig. 4 is the arched boundary of the sample.

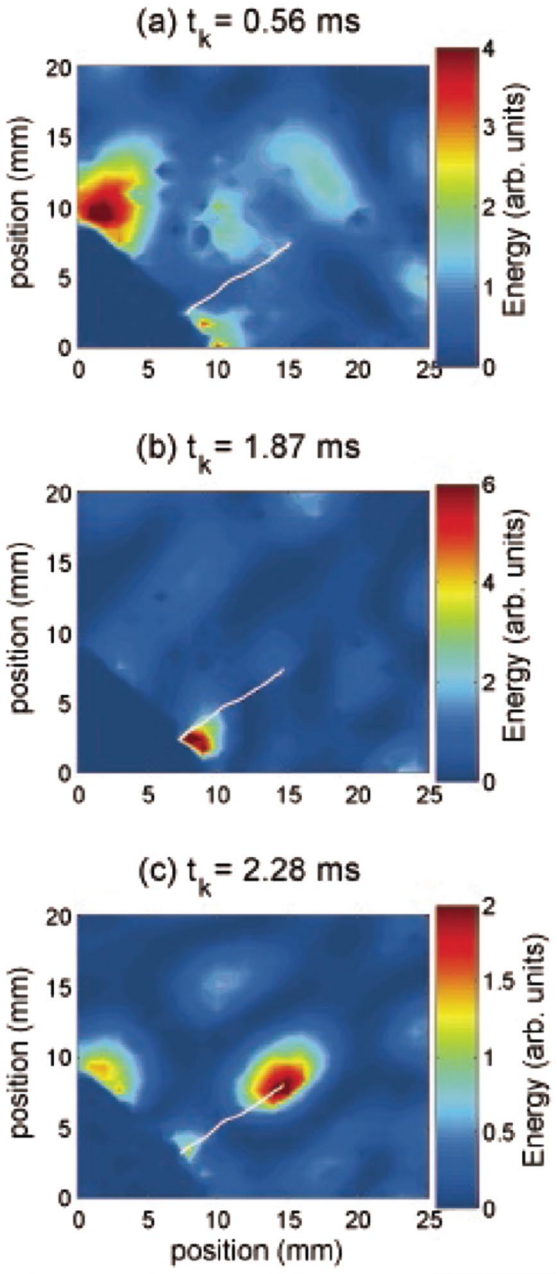

FIG. 4 (color). Elastic energy localization at time intervals $t_k - t_k + \Delta t$ (a) 0.56–0.62 ms (not focused on the nonlinear scatterer), (b) 1.87–1.93 ms (focused at one end on the nonlinear scatterer), and (c) 2.28–2.34 ms (focused at the opposite end of the nonlinear scatterer), illustrating the complex evolution of the energy refocusing onto the scatterer. The crack highlighted in white has been overlayed to show its location. The off-crack illumination may be due to geometrically controlled scattering of the time-reversed signal after it has refocused on the crack. For more illustration of the spatial-temporal complexity videos are available [13].

interactions. The source of nonlinear elasticity in mechanically damaged samples has been speculated to arise from asperity friction, crack "clapping," thermoelasticity, dislocation-point defect interaction, adhesion due to fluids, and possibly others. The method presented here may provide the means to support or dispute the above speculations or even spawn others. These are open questions we intend to explore in order to further understand the physical basis of the origins of nonlinear scattering in such a system.

Another goal of this research is remote imaging of isolated nonlinear scatterers. That is, here we directly image the surface of the sample over the region of the scatterer because we know where it is located and are able to directly access the feature at the surface of the sample. An internal scatterer located at an unknown position presents a more difficult problem. Our approach to this problem is to make the same lab measurement presented here, but back-propagate the filtered, time-reversed signal numerically in order to locate and image the internal nonlinear scatterer. This technique would require an experimentally obtained material velocity structure (i.e., travel time tomography), the direct signals $r_i(t)$ described herein, and a numerical model capable of properly utilizing the afore mentioned experimental data.

The work was supported by Institutional Support (LDRD) at the Los Alamos National Laboratory. The authors are grateful for invaluable input from J. TenCate and A. Sutin.

[1] R. A. Guyer and P. Johnson, Phys. Today **52**, No. 4, 30 (1999).
[2] P. A. Johnson and A. Sutin, J. Acoust. Soc Am. **117**, 124 (2005).
[3] P. A. Johnson, in Universality of Nonclassical Nonlinearity, edited by P. P. Delsanto and S. Hirsekorn (Springer, New York, to be published).
[4] K. E.-A. Van Den Abeele, P. A. Johnson, and A. Sutin, Research in Nondestructive Evaluation **12**, 17 (2000).
[5] V. V. Kazakov, A. Sutin, and P. A. Johnson, Appl. Phys. Lett. **81**, 646 (2002).
[6] L. A. Ostrovsky and P. Johnson, Riv. Nuovo Cimento **24**, 1 (2001).
[7] I. Solodov and G. Busse, Current Topics in Acoustical Research **3**, 163 (2003).
[8] I. Solodov, J. Wackerl, K. Pfleiderer, and G. Busse, Appl. Phys. Lett. **84**, 5386 (2004).
[9] M. Fink, Sci. Am. **281**, No. 5, 91 (1999).
[10] M. Tanter, J.-L. Thomas, F. Coulouvrat, and M. Fink, Phys. Rev. E **64**, 016602 (2001).
[11] *Nonlinear Acoustics*, edited by M. Hamilton and D. T. Blackstock (Academic, New York, 1997); L. Naugolnykh and L. Ostrovsky, *Nonlinear Wave Processes in Acoustics* (Cambridge University Press, Cambridge, England, 1998).
[12] L. D. Landau and E. M. Lifschitz, *Theory of Elasticity* (Pergamon, New York, 1986).
[13] See EPAPS Document No. E-PRLTAO-98-060710 for a video showing elastic energy focusing on the nonlinear scatterer for $f_- = 200$ kHz. For more information on EPAPS, see http://www.aip.org/pubservs/epaps.html.